Matter-wave diffraction in time with a linear potential

2006 J. Phys. A: Math. Gen. 39 5897

(http://iopscience.iop.org/0305-4470/39/20/017)

INSTITUTE OF PHYSICS PUBLISHING JOURNAL OF PHYSICS A: MATHEMATICAL AND GENERAL

J. Phys. A: Math. Gen. **39** (2006) 5897–5906 doi:10.1088/0305-4470/39/20/017

Matter-wave diffraction in time with a linear potential

A del Campo and J G Muga

Departamento de Química-Física, Universidad del País Vasco, Apdo. 644, Bilbao, Spain

E-mail: qfbdeeca@ehu.es and jg.muga@ehu.es

Received 8 March 2006
Published 3 May 2006
Online at stacks.iop.org/JPhysA/39/5897

Abstract

Diffraction in time of matter waves incident on a shutter which is removed at time $t = 0$ is studied in the presence of a linear potential. The solution is also discussed in phase space in terms of the Wigner function. An alternative configuration relevant to the current experiments where particles are released from a hard-wall trap is also analysed for single-particle states and for a Tonks–Girardeau gas.

PACS numbers: 03.75.−b, 03.75.Be, 03.75.Kk

1. Introduction

Diffraction in time (DIT) was studied first by Moshinsky [1, 2], and a flurry of both experimental and theoretical work investigating similar transient effects and setups has been carried out ever since. (For a brief recent review, see [3].) Quantum temporal oscillations of matter waves released from a shutter or confinement region constitute the hallmark of the effect.

Remarkably, all the theoretical studies have dealt with the quantum dynamics in free space or potentials with finite support [4–6]. However, the presence of a linear potential is ineludible for some experimental setups. This is actually the case for the first experimental observation of DIT, which made an explicit use of gravity on a system of ultracold atoms [7, 8]. Gravitational effects are also crucial in cold atom fountains as those used for frequency standards [9]. In addition, a linear potential arises from the interaction of a charged particle with an electric field, but it is within the field of atom optics that linear potentials, generally created by a magnetic field, have received a great deal of attention for ultracold atom manipulation, as a plugging potential for loading schemes, or aimed to cloud focusing, cooling and other key operations [10, 11].

One of the natural configurations to deal with such situations in a stationary regime, namely that of a point-like and Gaussian sources, has already been discussed in excellent agreement with photo-detachment and atom-laser experiment [12]. In this work we generalize the Moshinsky shutter problem, i.e. a cut-off plane wave released at time $t = 0$, by turning

on a linear potential at that instant. The exact solution is derived in section 3 together with its Wigner function. A related configuration, namely, that of particles initially trapped in a rectangular box is analysed in section 4. The experimental build-up of all-optical hard-wall traps [13] has excited a great deal of attention for such geometries both at single [14, 15] and many-particle levels [16–19]. In particular, experiments are in view to study the quantum dynamics in the Tonks–Girardeau (TG) regime with Fock states of a low particle number, N [20]. The experimental observation of DIT with a Bose–Einstein condensate [21] is in good agreement with the dynamics entailed in the time-dependent Schrödinger equation, showing that the condensate evolves as a free non-interacting particle gas after few milliseconds of expansion. Indeed, the importance of nonlinearity during free expansion has been studied in full detail for the case of the Tonks–Girardeau gas in [19] and shown to dominate in a time scale shorter than $t_N = mL^2/(2N\pi\hbar)$, L being the size of the initial trap and m the mass of the particle. The expansion of the Tonks–Girardeau gas will be analysed in section 5.

2. Diffraction in time in free space

The paradigmatic setup for DIT corresponds to a beam of particles incident on a shutter represented by an infinite potential barrier. The relevance on the diffraction pattern of the reflectivity of the barrier [1] as well as different types of beams has been thoroughly investigated in [3]. For simplicity, we will assume here a totally absorbing barrier so that the initial state is given by a cut-off plane wave:

$$\psi(x, t = 0) = \mathrm{e}^{\mathrm{i}px/\hbar}\Theta(-x). \tag{1}$$

The solution to the time dependent Schrödinger equation [1, 2] reads

$$\psi(x, t) = M(x, p/\hbar, \hbar t/m) := \frac{\mathrm{e}^{\mathrm{i}\frac{mx^2}{2t\hbar}}}{2} w(-z), \tag{2}$$

with

$$z = \frac{1+\mathrm{i}}{2}\sqrt{\frac{t}{m\hbar}}\left(p - \frac{mx}{t}\right), \tag{3}$$

and the so-called Faddeyeva function [22, 23] w is defined as

$$w(z) := \mathrm{e}^{-z^2}\mathrm{erfc}(-\mathrm{i}z) = \frac{1}{\mathrm{i}\pi}\int_{\Gamma_-} \mathrm{d}u \frac{\mathrm{e}^{-u^2}}{u - z}, \tag{4}$$

where Γ_- is a contour in the complex z-plane which goes from $-\infty$ to ∞ passing below the pole. After [1, 24], $M(x, k, t)$ has been named the Moshinsky function. At variance with the classical solution, the probability density presents genuine quantum oscillations in time and space. Note that a point of constant probability P propagates as

$$x_P(t) = \frac{pt}{m} - \sqrt{\frac{\pi\hbar t}{m}}u_{0,P}, \tag{5}$$

$u_{0,P}$ being a given constant. This result will be compared with the case where the evolution takes place in the presence of a linear potential.

3. Diffraction in time with a linear potential

We next study DIT in the presence of a linear potential. Consider a beam of particles incident from the left as before on a totally absorbing shutter located at the position $x = 0$, see (1). Suddenly, the shutter is removed at time equal to zero, and a linear potential is switched

on. Such a model can simulate the quantum dynamics of a confined charged particle, with a homogeneous electric field turned on at the time when the infinite potential wall at the origin is removed. Also, it can be applied to a particle in a gravitational field; in that case the cut-off plane wave may be used as a basis element to describe the actual initial state.

The evolved wavefunction obeys the integral equation

$$\psi(x,t) = \int_{-\infty}^{\infty} \mathrm{d}x' K(x,t|x',0)\psi(x',0), \tag{6}$$

where $K(x,t|x',t')$ is the propagator for a Hamiltonian with a general linear potential of the form

$$\hat{H} = \frac{p^2}{2m} + fx, \tag{7}$$

with f the constant. It is indeed well known [25],

$$K(x,t|x',t') = \sqrt{\frac{m}{2\pi \mathrm{i}\hbar(t-t')}} \exp\left(\mathrm{i}\frac{m(x-x')^2}{2\hbar(t-t')} - \mathrm{i}\frac{f(x+x')(t-t')}{2\hbar} - \mathrm{i}\frac{f^2(t-t')^3}{24\hbar}\right), \tag{8}$$

and related to the action of the classical path.

Inserting (8) into (6), we find

$$\psi(x,t) = \sqrt{\frac{m}{2\pi \mathrm{i}\hbar t}} \exp\left(-\mathrm{i}\frac{f^2t^3}{24\hbar} - \mathrm{i}\frac{ftx}{2\hbar}\right) \int_{-\infty}^{0} \mathrm{d}x' \exp\left(\mathrm{i}\frac{m(x-x')^2}{2\hbar t} + \mathrm{i}(p - ft/2)x'/\hbar\right). \tag{9}$$

It is convenient to introduce the auxiliary variables

$$\begin{aligned} u &\equiv \sqrt{\frac{m}{\pi t\hbar}}(x'-x) + \sqrt{\frac{t}{\pi m\hbar}}(p - ft/2), \\ u_0 &\equiv \sqrt{\frac{t}{\pi m\hbar}}(p - ft/2) - \sqrt{\frac{m}{\pi t\hbar}}x, \end{aligned} \tag{10}$$

to write (9) as

$$\psi(x,t) = \frac{1}{\sqrt{2\mathrm{i}}} \exp\left(-\mathrm{i}\frac{f^2t^3}{24\hbar} - \mathrm{i}\frac{ftx}{2\hbar}\right) \int_{-\infty}^{u_0} \mathrm{d}u \exp\left(\mathrm{i}\frac{\pi u^2}{2}\right), \tag{11}$$

which can be expressed in terms of the Fresnel sine and cosine integrals,

$$\int_{-\infty}^{u_0} \mathrm{d}u\, \mathrm{e}^{\mathrm{i}\frac{\pi u^2}{2}} = \frac{1+\mathrm{i}}{2} + \int_{0}^{u_0} \mathrm{d}u\, \mathrm{e}^{\mathrm{i}\frac{\pi u^2}{2}} = \frac{1+\mathrm{i}}{2} + C(u_0) + \mathrm{i}S(u_0). \tag{12}$$

From the last equation, it is possible to map the probability density to the Cornu spiral [1]. Additionally, the following relation between the Fresnel integrals and the w function holds [23]:

$$C(u_0) + \mathrm{i}S(u_0) = \frac{1+\mathrm{i}}{2}\left(1 - \mathrm{e}^{\mathrm{i}\frac{\pi u_0^2}{2}} w\left[\frac{\sqrt{\pi}}{2}(1+\mathrm{i})u_0\right]\right). \tag{13}$$

Then, one can make use of Faddeyeva's identity, which follows from the Cauchy theorem,

$$w(z) + w(-z) = 2\mathrm{e}^{-z^2}, \tag{14}$$

to end up with the result

$$\psi(x,t) = \frac{1}{2} \exp\left(-\mathrm{i}\frac{f^2t^3}{24\hbar} - \mathrm{i}\frac{ftx}{2\hbar} + \mathrm{i}\frac{mx^2}{2m\hbar}\right) w(-z), \tag{15}$$

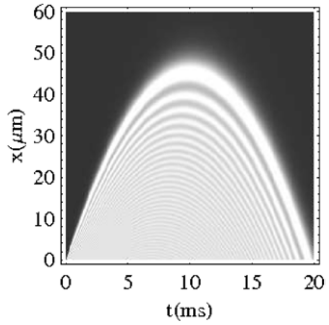

Figure 1. Probability density on the $t - x$ plane, which clearly shows the diffraction in time and space for an incident beam of rubidium atoms in a fountain configuration ($p/m = 1$ cm s^{-1}, $f/m = 0.1 * g$). The grey scale changes from light to dark as the function values decrease. The same colour coding is used in all density plots.

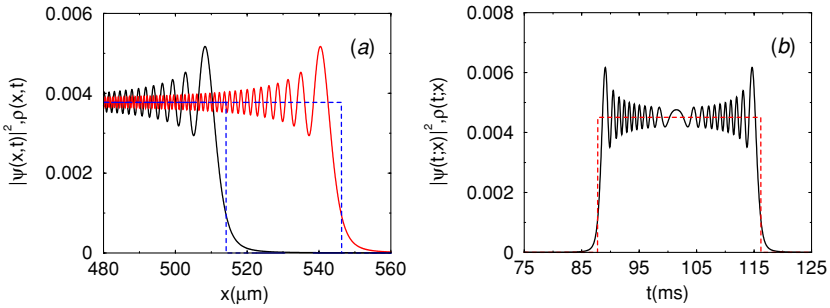

Figure 2. (a) Probability density for both free and accelerated beams at $x > 0$ with $p/m = 5$ cm s^{-1}, $f/m = -0.1$ cm s^{-2} (solid lines) and the corresponding classical density (dashed lines) 10 ms after removing the shutter ($m = m_{\mathrm{Rb}}$ in all the calculations). (b) The diffraction in time for an incident beam with $p/m = 10$ cm s^{-1} registered by a detector located at 5 mm from the shutter, $f/m = 0.05$ cm s^{-2}. The dashed line corresponds to the classical density.

(This figure is in colour only in the electronic version)

where now

$$z \equiv \frac{1+\mathrm{i}}{2}\sqrt{\frac{t}{m\hbar}}\left(p - \frac{ft}{2} - \frac{mx}{t}\right). \tag{16}$$

In figure 1 a contour diagram of the probability density on the plane $t - x$ is plotted for a 'fountain configuration', namely, for the case in which the initial velocity goes in the direction of an increasing potential. In such a representation, it is particularly easy to appreciate the diffraction in both time and space domains.

To learn about the main features of this solution, we compare it in figure 2 with the free case. Indeed, it is amusing to rewrite (15) in terms of the Moshinsky function as

$$\psi(x,t) = \exp\left(-\mathrm{i}\frac{f^2t^3}{6m\hbar} + \mathrm{i}\frac{ftx}{\hbar}\right) M\left(x - \frac{ft^2}{2m}, \frac{p}{\hbar}, \frac{\hbar t}{m}\right), \tag{17}$$

which exactly reduces to the result of section 2 for $f = 0$. Note that the dynamics is modified with respect to the free particle case by correcting both momentum and position with the classically expected time-dependent canonical transformation, as shown in figure 2(a), up to

an additional phase. In fact, the main difference is that, for a given u the equation of motion for the associated point of constant probability, and in particular for the maximum and minimum, can be deduced to be

$$x_{\max}(t) = \frac{pt}{m} - \frac{ft^2}{2m} - \sqrt{\frac{\pi\hbar t}{m}}u_{0,\max}, \tag{18}$$

$$x_{\min}(t) = \frac{pt}{m} - \frac{ft^2}{2m} - \sqrt{\frac{\pi\hbar t}{m}}u_{0,\min}, \tag{19}$$

where $u_{\max} = 1.2172$ and $u_{\min} = 1.8725$ are universal for the cut-off plane wave case considered here. From these equations, the turning point in figure 2 can be inferred.

As stated above, the telltale sign of DIT is a set of oscillations, observed after removing the shutter, in the probability density and which are genuinely quantum in nature. For the diffraction in time with a linear potential, the fringe visibility

$$\mathcal{V}(T) = \frac{P_{1\text{st max}} - P_{1\text{st min}}}{P_{1\text{st max}} + P_{1\text{st min}}} \tag{20}$$

turns out to be independent of time, for the quasi-monochromatic case, as in the absence of the external field.

As pointed out before, the diffraction in time also admits a representation of the Cornu spiral. The classical probability density, given by a step function, intersects the quantum one at two different points. Therefore, an estimate of the width for the largest fringe can be carried out by considering the intersection with the classical probability density. The same result without linear potential then holds,

$$\Delta x \simeq 0.85\sqrt{\frac{\pi\hbar t}{m}} \tag{21}$$

[1, 2], provided that the probability is exclusively u-dependent, as should be clear from (11), $P_{\max} = 1.370$; $P_{\min} = 0.778$. An alternative representation which explicitly exhibits the diffraction pattern in the time domain is shown in figure 2(*b*), where the position of the detector is fixed and the signal of the incident beam is recorded as a function of time. One should note the similarity with the profile in a coordinate representation obtained by releasing a particle from a hard-wall trap with $f = 0$. This configuration was identified as the analogue of the diffraction in time from a slit in free space [15]. Nevertheless, due to the dispersion entailed in (21) the pulse registered in the time domain is not symmetric.

3.1. Wigner transform

The Wigner function [26],

$$\mathcal{W}(x, p) := \frac{1}{\pi\hbar}\int_{-\infty}^{\infty} \mathrm{d}y\, \psi(x+y)^*\psi(x-y)\, \mathrm{e}^{2\mathrm{i}py/\hbar}, \tag{22}$$

is the best known quasi-joint probability distribution for position and momentum. Nowadays, it is possible to study it experimentally as has been demonstrated in a series of works [27]. In the context of the Moshinsky shutter, its time evolution was derived for the free case problem in [28]. From that result at $t = 0^+$ or definition (22), it follows that for the cut-off plane wave initial condition, the Wigner function reads

$$\mathcal{W}(x, p; p_0, t = 0^+) = \frac{1}{\pi}\frac{\sin[-2x(p_0 - p)/\hbar]}{p_0 - p}\Theta(-x), \tag{23}$$

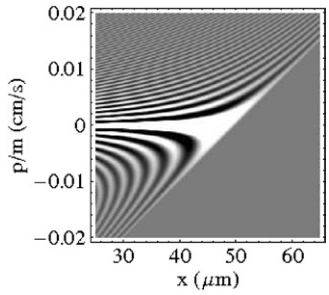

Figure 3. The Wigner function for the atom fountain configuration at the classical turning point ($p_0/m = 1$ cm s^{-1}, $f/m = 100$ cm s^{-2}, $t = 10$ ms). The grey triangle at the lower-right corner is the classically unaccessible region for which $\mathcal{W}(x, p; t) = 0$.

which clearly assumes negative values. For potentials of degree $n = 2$ at the most, the time-evolved Wigner function follows the classical trajectories:

$$\mathcal{W}(x, p; t) = \iint \mathrm{d}x_0\, \mathrm{d}p_0\, \delta[x - x_{\mathrm{cl}}(x_0, p_0, t)]\, \delta[p - p_{\mathrm{cl}}(x_0, p_0, t)] \mathcal{W}(x, p; t = 0). \tag{24}$$

Alternatively, one can cope with the more cumbersome calculation starting from the definition as in [28]. For (15) the result is

$$\mathcal{W}(x, p; p_0, t) = \frac{\sin\left\{\frac{2}{\hbar}\left(\frac{pt}{m} + \frac{ft^2}{2m} - x\right)(p_0 - ft - p)\right\}}{\pi(p_0 - ft - p)} \Theta\left(\frac{pt}{m} + \frac{ft^2}{2m} - x\right). \tag{25}$$

Figure 3 shows the Wigner function calculated for an incident beam exactly at the classical turning point, being thus centred around $p = 0$. Note that, thanks to the step function, it is limited to the classically accessible region of the phase space. Indeed, following [28] we can ask for the classical limit taking $\hbar \to 0$ to find

$$\mathcal{W}_{\mathrm{cl}}(x, p; p_0, t) = \delta(p_0 - ft - p)\Theta\left(\frac{p_0 t}{m} - \frac{ft^2}{2m} - x\right). \tag{26}$$

As expected, the correct classical equation of motion $x = x_{\mathrm{cl}}(t)$, $p = p_{\mathrm{cl}}(t)$ is recovered and no hint about the quantum oscillations—hallmark feature of DIT—remains.

4. The hard-wall trap

In this section we consider the dynamics of a particle initially confined in a box. At time zero, its walls are suddenly removed and a linear potential is switched on. The paradigmatic particle in a box (PIAB) has been recently implemented in an all-optical fashion by Raizen *et al* [13] with a Bose–Einstein condensate, and experiments are in view with Fock states of a low number of particles, $N < 10$ [20]. From the theoretical point of view, the free evolution of the wavefunction which results after shutting off the walls was discussed a long time ago within the context of ultracold neutrons interferometry [14]. Later, it was reformulated by Godoy [15], who pointed out the analogy with the Fraunhoffer diffraction in the case of a small box (compared to the de Broglie length), and Fresnel diffraction, for larger confinements. Quite recently, a generalization to an interacting many-body system was investigated in the regime of a Tonks–Girardeau gas [19].

If $\chi_{[0,L]}(z)$ is the characteristic function in the interval $[0, L]$, let us now consider the initial condition given by an arbitrary excited state $|\psi_n\rangle$:

$$\psi_n(x,t) = \sqrt{\frac{2}{L}} \sin\left(\frac{n\pi x}{L}\right) \chi_{[0,L]}(x). \tag{27}$$

Using the decomposition of the characteristic function $\chi_{[0,L]}(x) = \Theta(L-x) - \Theta(-x)$, the $\psi_n(x,t)$ term can be worked out to be

$$\psi_n(x,t) = \sqrt{\frac{m}{2\pi \mathrm{i}\hbar t}} \exp\left(-\mathrm{i}\frac{ftx}{2\hbar} + \mathrm{i}\frac{ft^2}{24\hbar}\right) \sum_{\alpha=\pm} \alpha \left[\int_{-\infty}^{L} \mathrm{d}x' \exp\left(\mathrm{i}\frac{m(x-x')^2}{2\hbar t} + \mathrm{i}\frac{p_\alpha x'}{2\hbar}\right)\right.$$
$$\left. - \int_{-\infty}^{0} \mathrm{d}x' \exp\left(\mathrm{i}\frac{m(x-x')^2}{2\hbar t} + \mathrm{i}\frac{p_\alpha x'}{\hbar}\right)\right], \tag{28}$$

where we have defined

$$p_\alpha \equiv \frac{\alpha\hbar n\pi}{L} - \frac{ft}{2}. \tag{29}$$

Carrying similar steps to the ones described for the previous section, one finally ends up with

$$\psi_n(x,t) = \frac{1}{4\mathrm{i}}\sqrt{\frac{2}{L}} \exp\left(-\mathrm{i}\frac{ftx}{2\hbar} + \mathrm{i}\frac{ft^2}{24\hbar}\right) \sum_{\alpha=\pm} \alpha \left[\exp\left(\mathrm{i}\frac{p_\alpha L}{\hbar} + \mathrm{i}\frac{m(x-L)^2}{2\hbar t}\right)\right.$$
$$\left. \times w(-u_{\alpha L}) - \exp\left(\mathrm{i}\frac{mx^2}{2\hbar t}\right) w(-u_{\alpha 0})\right], \tag{30}$$

where

$$u_{\alpha L} = \frac{1+\mathrm{i}}{2}\sqrt{\frac{t}{m\hbar}}\left(p_\alpha - \frac{m(x-L)}{t}\right), \qquad u_{\alpha 0} = \frac{1+i}{2}\sqrt{\frac{t}{m\hbar}}\left(p_\alpha - \frac{mx}{t}\right). \tag{31}$$

In an atomic fountain, trapped atoms are launched vertically with the help of the optical molasses technique. PIAB eigenstates are a good approximation to the actual state of a box subjected to a linear potential, whenever the box is small and the particle is light. Indeed, within a first-order perturbation theory, the coefficients C_{nk} responsible for the corrections on the nth eigenstate $\left(\left|\phi_n^{(1)}\right\rangle = \left|\phi_n^{(0)}\right\rangle + \sum_{k\neq n} C_{nk}\left|\phi_k^{(0)}\right\rangle\right)$ due to the linear potential are given by

$$C_{nk} = \frac{8mfL^3}{\hbar^2\pi^4}\frac{nk[(-1)^{n+k}-1]}{k^2-n^2}. \tag{32}$$

If the perturbation of the initial state by the linear potential is significant, it can always be written as a linear combination of the eigenstates of the free Hamiltonian within the box, namely, $\{\phi_n(x) = \sqrt{2/L}\sin(n\pi x/L)|n \in \mathbb{N}\}$. We must therefore look for the evolution of a PIAB state released at time $t = 0$ and launched with a given momentum q. Explicitly, it is described by (30), with the redefinition

$$p_\alpha \equiv q + \frac{\alpha\hbar n\pi}{L} - \frac{ft}{2}. \tag{33}$$

Equation (30) can also model the output coupling mechanism of an atom laser. In such devices, an atom is initially in the lasing mode, confined by the cavity mirrors which can be simulated by two infinite walls (reducing the problem to that of a PIAB). Through a Raman transition, this atom evolves to a nontrapped state, which amounts to shutting off the walls. During the transition and due to the emission of a photon, the atom is kicked with a given momentum, namely, q [29].

Figure 4 shows the time evolution of the density profile for the tenth eigenstate of the initial hard-wall trap. A most relevant feature is that at variance with the well-known

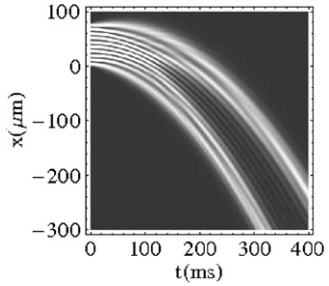

Figure 4. Time evolution of the density profile for an eigenstate of the hard-wall trap, with $n = 10$, $q = 0$ cm s^{-1}, $L = 80$ μm and $f/m = 0.49$ cm s^{-2}. Bifurcation for $t > t_{n=10} \simeq 137$ ms occurs in analogy with free case. This is the time that would take a point particle initially located at the centre of the trap to reach one of the edges when moving with $p_{10} = 10\hbar\pi/L$. The expectation value $\langle\hat{x}(t)\rangle$ reproduces the classical trajectory.

harmonic trap case, the profile bifurcates into two main branches after the semiclassical time $t_n = mL/(2p_n) = mL^2/(2n\pi\hbar)$. This behaviour has been recently reported for the free particle case by the authors [19] and holds for any excited state for both even and odd quantum numbers $n > 1$. The cloud falls under acceleration following $\langle\psi|\hat{x}(t)|\psi\rangle$ the classical trajectory, even though for any $t > t_n$ the probability is vanishing along with it.

5. Tonks gas dynamics in a linear potential

Under strong radial confinement and at low densities and temperatures, an ultracold atomic gas becomes effectively one dimensional. In particular, whenever the thermal and zero-point energies are lower than the transversal excitation quantum, the TG regime is reached. The effective interactions are then so strong that the gas behaves like a system of hard-core impenetrable bosons. Such a regime has been obtained in several experiments [30], and a full quantum description is possible, thanks to the Fermi–Bose mapping theorem [31]. According to it, the many-body wavefunction of a TG gas can be obtained from that of a zero-spin free fermionic gas, by applying the àntisymmetric unit function' $\mathcal{A} = \prod_{1\leqslant j<k\leqslant N} \mathrm{sgn}(x_k - x_j)$, as $\psi_B(x_1, \ldots, x_N; t) = \mathcal{A}(x_1, \ldots, x_N)\psi_F(x_1, \ldots, x_N; t)$. Indeed, one can state $|\psi_B(x_1, \ldots, x_N; t)|^2 = |\psi_F(x_1, \ldots, x_N; t)|^2$, for the mapping is involutive. The dual system to the TG gas, being the ideal Fermi system, is built up as a Slater determinant:

$$\psi_F(x_1, \ldots, x_N; t) = \frac{1}{\sqrt{N!}} \det_{n,k=1}^{N} \phi_n(x_k; t). \tag{34}$$

Moreover, thanks to the fact that under unitary time evolution, orthonormality between the initial eigenstates of the trap is preserved, it follows that any local correlation function can be obtained in a close form. For example, the calculation of the density profile is greatly simplified to

$$\varrho(x, t) = N\int |\psi_B(x, x_2, \ldots, x_N; t)|^2 \, \mathrm{d}x_2 \cdots \mathrm{d}x_N = \sum_{n=1}^{N} |\phi_n(x, t)|^2. \tag{35}$$

The free expansion dynamics of a TG gas from a hard-wall trap was recently considered in [19], where a dynamics much more complicated than for the harmonic confinement was observed. Taking advantage of the results obtained in the previous section, we next generalize the free expansion results and deal with the following experiment. Consider a TG gas initially

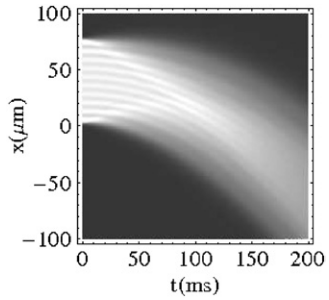

Figure 5. Time evolution of the density profile for a Tonks–Girardeau gas, with $N = 10$, $q = 0$ cm s^{-1}, $L = 80$ μm and $f/m = 0.49$ cm s^{-2}. The interference pattern is washed out for $t > t_{N=10} \simeq 137$ ms.

confined in a hard wall trap. At zero time it receives a momentum kick, the momentum at which the shutter is off and the linear potential rumped up. The density profile is found combining (30) and (35).

Figure 5 shows the density profile of the expanding cloud in space and time falling under the action of a linear potential. For short times $t < t_N$, there is a well-defined pattern where the number of maxima equals that of particles. After a transient regime where the visibility of the peaks varies in a non-trivial way, it is gradually lost for $t > t_N$. In the later regime, the ballistic expansion is established in agreement with the force-free case [19].

6. Conclusions

Diffraction in time has been generalized in the presence of a linear potential. Moreover, the dynamics of particles released from a hard-wall trap under a constant force has been studied, showing a bifurcation after a time $t_n = mL^2/(2n\pi\hbar)$, in analogy with the free case [19]. This is a novel feature exclusively associated with hard-wall traps. Note that for the case of harmonic confinement, the evolution follows a scaling law of coordinates, lacking therefore any transient effect [33]. In addition, the expansion of a Tonks–Girardeau gas has been exactly solved using the Bose-Fermi map. The cloud is shown to exhibit an interference pattern which is lost for $t > t_N$. Finally, we point out that any time dependence on the linear potential can be easily included using the general map obtained in [34]. In such a way, one can account for a smooth ramping up of the linear potential.

Acknowledgments

The papers has been benefited from discussions with A Ruschhaupt and M Rodriguez. This work has been supported by T Ministerio de Educación y Ciencia (BFM2003-01003) and UPV-EHU (00039.310-15968/2004). AC acknowledges financial support by the Basque Government (BFI04.479).

References

[1] Moshinsky M 1952 *Phys. Rev.* **88** 625
[2] Moshinsky M 1976 *Am. J. Phys.* **44** 1037
[3] del Campo A and Muga J G 2005 *J. Phys. A: Math. Gen.* **38** 9803

[4] Kleber M 1994 *Phys. Rep.* **236** 331
[5] García-Calderón G and Rubio A 1997 *Phys. Rev.* A **55** 3361
[6] García-Calderón G and Villavicencio J 2001 *Phys. Rev.* A **64** 012107
[7] Steane A, Szriftgiser P, Desbiolles P and Dalibard J 1995 *Phys. Rev. Lett.* **74** 4972
[8] Arndt A, Szriftgiser P, Dalibard J and Steane A M 1996 *Phys. Rev.* A **53** 3369
[9] Clairon A, Laurent P, Nadir A, Drewsen M, Grison D, Lounis B and Salomon C 1992 *EFTF: Proc. 6th European Frequency and Time Forum*
[10] Folman R, Krüger P and Schmiedmayer J 2002 *Adv. Atom. Mol. Opt. Phys.* **48** 263
[11] Metcalf H J and van der Straten P 1999 *Laser Coooling and Trapping* (New York: Springer)
[12] Kramer T, Bracher C and Kleber M 2002 *J. Phys. A: Math. Gen.* **35** 8361
Kramer T 2003 Matter waves from localized sources in homogeneous force fields http://tumb1.biblio.tu-muenchen.de/publ/diss/ph/2003/kramer.pdf and references therein
[13] Meyrath T P, Schreck F, Hanssen J L, Chuu C-S and Raizen M G 2005 *Phys. Rev.* A **R71** 041604
[14] Gerasimov A S and Kazarnovskii M V 1976 *Sov. Phys.—JETP* **44** 892
[15] Godoy S 2002 *Phys. Rev.* A **65** 042111
[16] Gaudin M 1971 *Phys. Rev.* A **4** 386
[17] Cazalilla M A 2002 *Europhys. Lett.* **59** 793
Cazalilla M A 2004 *J. Phys. B: At. Mol. Opt. Phys.* **37** S1
[18] Batchelor M T, Guan X W, Oelkers N and Lee C 2005 *J. Phys. A: Math. Gen.* **38** 7787
[19] del Campo A and Muga J G 2005 *Preprint* cond-mat/0511747
[20] Raizen M G 2005 Personal communications
[21] Colombe Y, Mercier B, Perrin H and Lorent V 2005 *Phys. Rev.* A **72** 061601
[22] Faddeyeva V N and Terentev N M 1961 *Mathematical Tables: Tables of the Values of the Function $w(z)$ for Complex Argument* (New York: Pergamon)
[23] Abramowitz A and Stegun I A 1965 *Handbook of Mathematical Functions* (New York: Dover)
[24] Moshinsky M 1951 *Phys. Rev.* A **84** 525
[25] Grosche C and Steiner F 1998 *Handbook of Feynman Path Integrals (Springer Tracts in Modern Physics* vol 145) (Berlin: Springer)
[26] Wigner E P 1932 *Phys. Rev.* **40** 749
[27] Smithey D T *et al* 1993 *Phys. Rev. Lett.* **70** 1244
Leibfried D *et al* 1996 *Phys. Rev. Lett.* **77** 4281
Breitenbach G, Schiller S and Mlynek J 1997 *Nature* **387** 471
Kurtsiefer Ch, Pfau T and Mlynek J 1997 *Nature* **386** 150
Lvovsky A I *et al* 2001 *Phys. Rev. Lett.* **87** 050402
Lougovski P *et al* 2003 *Phys. Rev. Lett.* **91** 010401
[28] Mánko V, Moshinsky M and Sharma A 1999 *Phys. Rev.* A **59** 1809
[29] Hagley E W *et al* 1999 *Science* **283** 1706
[30] Paredes B *et al* 2004 *Nature* **429** 227
Kinoshita T, Wenger T and Weiss D 2004 *Science* **305** 1125
[31] Girardeau M 1960 *J. Math. Phys.* **1** 516
[32] Brouard S and Muga J G 1996 *Phys. Rev.* A **54** 3055
[33] Perelomov A M and Zel'dovich Y B 1998 *Quantum Mechanics: Selected Topics* (Singapore: World Scientific)
[34] Song D Y 2003 *Europhys. Lett.* **65** 622